# Effect of near-fault long-period ground motions on seismic response of base-isolated structures

2017 NZSEE Conference

J. Ma, C.H. Sun & J. Ge

*Engineering Research Institute, China Construction Eighth Engineering Division Co., Ltd., Shanghai.*

D. Ning, L.M. Qing & X.L. Yang

*Northwest Branch Company, China Construction Eighth Engineering Division Co., Ltd., Xi'an.*

**ABSTRACT:** This paper presents a comparison of the expected seismic performance of a base-isolated hospital building considering near-fault long-period and ordinary ground motions. A five-story base-isolated RC frame hospital building with Lead rubber bearings and Natural rubber bearings is selected in this study. Twelve near-fault long-period earthquake records from Chi-Chi earthquake (Sep., 21, 1999) and Loma Prieta earthquake (Oct., 17, 1989), and four ordinary earthquake records determined according to current Chinese seismic code are selected as the input excitations. Nonlinear time history analysis is conducted, and the predicted dynamic responses including peak story displacements, peak story shear forces, and the restoring force characteristics in the base isolation layer under near-fault long-period ground motions are compared with those of ordinary ground motions. The results demonstrate that near-fault long-period ground motions can lead to larger story displacements and story shear forces on the base-isolated structure, and the base isolation layer dissipates more input earthquake energy when long-period ground motions are considered. The findings in the study indicate that higher seismic demands are expected when seismically isolated structures are subjected to near-fault long-period motions, and the long-period ground motions should be considered in structural design of seismically isolated buildings.

## 1 INTRODUCTION

Seismic isolation is recognized as an effective technique in protecting civil engineering structures, their functions and their occupants from seismic hazard, and has been increasingly used in China, Japan, and other earthquake-prone areas. The main feature of seismic isolation is that an isolation layer is introduced between the superstructure and the ground, thus fundamental natural period of the structure is shifted to the long period range, and the superstructure is decoupled from the harmful ground motions to reduce peak responses.

However, the significant effect of seismic isolation in reducing structural response is observed based on the fact that seismic isolation is effective for ground motions including mainly high-frequency components. In recent years, the viability of seismic isolation is reconsidered in the case where the design ground motions contain long-period components, and it is expected that long-period (1-10s or longer) ground motions can induce unacceptably large seismic demands on seismically isolated structures. Long-period ground motions are different from ordinary ground motions in that they often contain long dominant periods and long durations, thus they can induce particularly large seismic demands on long-period structures, such as high-rise buildings, long-span bridges, liquid storage tanks, as well as seismically isolated structures (Hall et al., 1995; Heaton et al., 1995; Malhotra, 1999; Jangid and Kelly, 2001; Shekari et al., 2010; Mazza and Vulcano, 2012). Therefore, the characteristics of seismic isolation needs to be re-examined when seismically isolated structures are subjected to long-period ground motions.

In this paper, the dynamic behavior of a base-isolated RC frame hospital building subjected to near-fault long-period ground motions is investigated in order to attain more insight on the effect of long-period seismic motions on seismically isolated structures. Twelve near-fault long-period ground motions and four ordinary ground motion are selected as the input excitations. A seismic evaluation of the base-isolated building is performed using nonlinear time history analysis, and seismic responses with respect to story displacements, story shear forces, and the restoring force characteristics of the base isolation layer are compared according to near-fault long-period ground motions and ordinary input motions. The purpose of this study is expected to further the understanding of the effects of long-period ground motions on seismic responses of seismically isolated structures, and to evaluate the adequacy of current design practices.

## 2 THE BASE-ISOLATED BUILDING

The Lanzhou Cancer Hospital Outpatient Building is a base-isolated five-storey reinforced concrete frame building, and consists of a basement and a base isolation layer underground, and five stories above the ground. The overview of the building is shown in Figure 1. The proportions of the structure at plan are 78.6 m and 70.2 m, and the story heights are listed as follows: Basement, 5.0 m; Base isolation (BI) layer, 2.0 m; First to Forth story, 4.95 m; Fifth story, 3.6 m. The lateral force-resisting system of the building is concrete moment frames in both transverse and longitudinal directions. Lightweight blocks are used as exterior walls. The building is located in the Lanzhou - Tianshui seismic zone, and hence may be subjected to significant ground shakings. The seismic fortification intensity in Lanzhou region is 8, and the basic peak ground acceleration is 0.2g.

A base isolation layer is introduced between the basement and the first story slabs, the height of the base isolation layer is from -2.0 m to the ground, as shown in Figure 2. A total of 140 rubber isolators are used in the base isolation layer, including 66 Lead rubber bearings (LRBs) and 74 Natural rubber bearings (NRBs). The diameter of rubber isolators is from 0.6 m to 0.9 m, and the total rubber height is from 0.12 m to 0.18 m. The rubber isolators are located at the center of columns, and 0.6 m above the top slabs of the basement. The mechanical properties of LRBs and NRBs are listed in Table 1, and the layout of the rubber isolators is shown in Figure 3.

Figure 1. Overview of the base-isolated building.

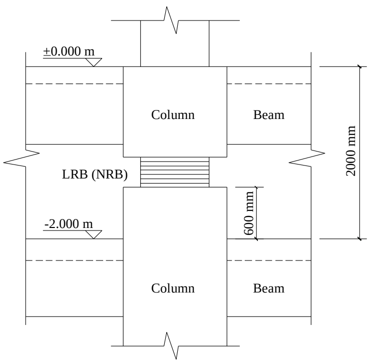

Figure 2. Base isolation layer.

**Table 1. Properties of Lead rubber bearings and Natural rubber bearings.**

| Type | Diameter (mm) | Rubber Height (mm) | $S_1$ | $S_2$ | Shear Modulus ($N/mm^2$) | Vertical Stiffness (kN/mm) | Effective Horizontal Stiffness (kN/m) | Effective Damping (%) |
|---|---|---|---|---|---|---|---|---|
| LRB600 | 600 | 120 | 27.5 | 5.0 | 0.4 | 2160 | 1520 | 24.5 |
| LRB700 | 700 | 140 | 31.3 | 5.0 | 0.4 | 2880 | 1760 | 24.0 |
| LRB800 | 800 | 160 | 31.3 | 5.0 | 0.55 | 3750 | 2900 | 25.5 |
| LRB900 | 900 | 180 | 31.3 | 5.0 | 0.4 | 4345 | 2300 | 25.2 |
| NRB600 | 600 | 120 | 27.5 | 5.0 | 0.4 | 2035 | 933 | 5.0 |
| NRB700 | 700 | 140 | 31.3 | 5.0 | 0.4 | 2730 | 1088 | 5.0 |

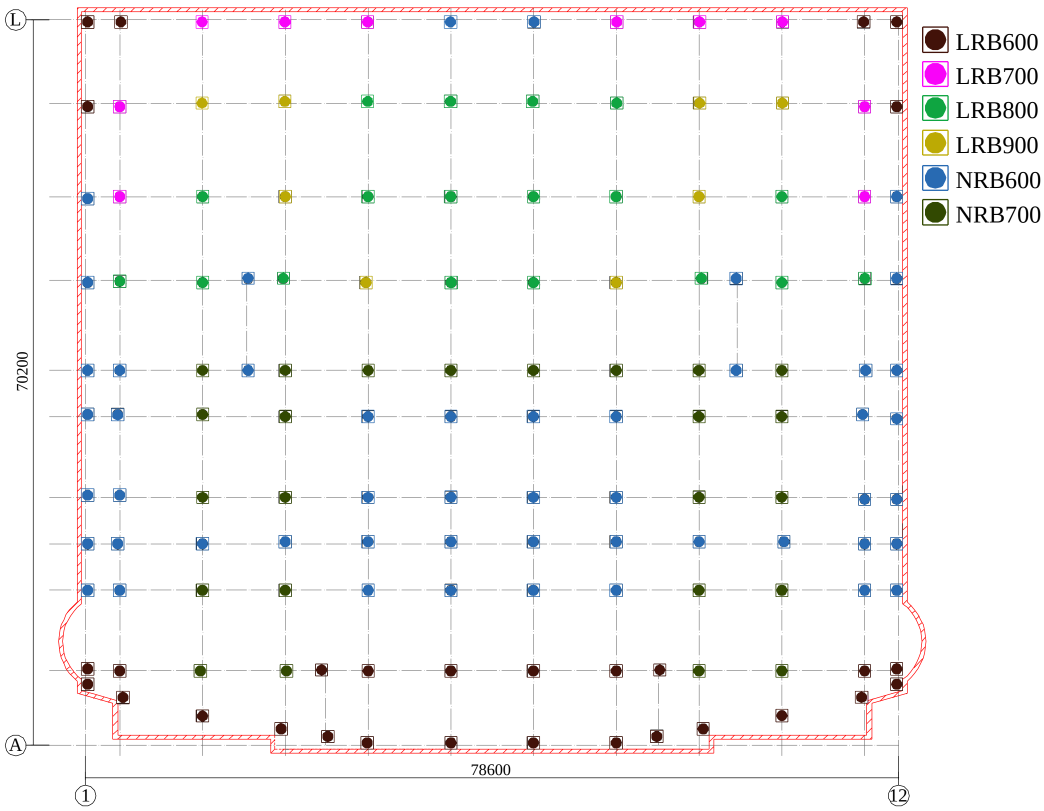

Figure 3. Layout of rubber isolators.

## 3 NEAR-FAULT LONG-PERIOD GROUND MOTIONS

Near-fault long-period ground motion represents a typical type of long-period ground motion, and its effect on seismically isolated structures have raised special attentions in recent studies (Liao et al., 2004; Dicleli et al., 2007). In this study, a total of twelve near-fault long-period ground motions are selected as input long-period ground motions, including eight records from Chi-Chi earthquake (Sep., 21, 1999) and four earthquake records from Loma Prieta earthquake (Oct., 17, 1989). The selected records characterizing near-fault long-period ground motions are larger than magnitude 6, and are obtained from the distance less than 20 km to the epicenter. Moreover, the dominant periods of the selected long-period records are larger than 1s. The peak ground acceleration (PGA), peak ground velocity (PGV), peak ground displacement (PGD), station number, and the closest distance from the station to the fault of each record are listed in Table 2. The data of selected records are obtained from the Center for Engineering Strong Motion Data (http://strongmotioncenter.org/).

Figure 4 illustrates the velocity spectra of the selected near-fault long-period ground motions for damping ratio of 0.05. It can be observed that the selected ground motions contain significantly long-period components and the dominant periods of these motions are larger than 1s. The high responses in the velocity response spectrum indicate that the selected near-fault long-period motions contain high-energy pulses, therefore large seismic demands are expected when long-period structures are subjected to these selected motions.

In addition, in order to evaluate the effects of near-fault long-period ground motions on seismic performance of the base-isolated structure, four ordinary earthquake records including EI Centro, Taft, Kobe, and Wenchuan earthquake records are determined according to current Chinese seismic code (GB 50011-2010) for the purpose of comparison.

**Table 2. Characteristics of selected near-fault long-period ground motions.**

| Earthquake | $M_W$ | Date | Station | Distance to Fault (km) | Comp. | PGA ($cm/s^2$) | PGV (cm/s) | PGD (cm/s) |
|---|---|---|---|---|---|---|---|---|
| Chi-Chi | 7.6 | 1999/09/21 | CHY024 | 9.3 | 90 | 276.2 | 50.7 | 39.9 |
| | | | TCU052 | 1.8 | 90 | 352.2 | 136.0 | 164.1 |
| | | | TCU053 | 5.5 | 90 | 224.3 | 33.6 | 37.4 |
| | | | TCU067 | 1.1 | 90 | 491.4 | 80.8 | 55.9 |
| | | | TCU068 | 3 | 90 | 494.4 | 213.3 | 186.5 |
| | | | TCU075 | 3.4 | 90 | 324.8 | 102.0 | 77.8 |
| | | | TCU102 | 1.2 | 90 | 297.1 | 90.2 | 91.0 |
| | | | TCU138 | 11.3 | 90 | 201.5 | 36.4 | 26.3 |
| Loma Prieta | 6.9 | 1989/10/17 | CSMIP47125 | 15.9 | 0 | 462.9 | 36.1 | 11.0 |
| | | | CSMIP47380 | 4.5 | 90 | 316.3 | 39.2 | 10.9 |
| | | | CSMIP58065 | 4.1 | 0 | 494.5 | 41.3 | 15.9 |
| | | | CSMIP58065 | 4.1 | 90 | 316.2 | 43.6 | 28.0 |

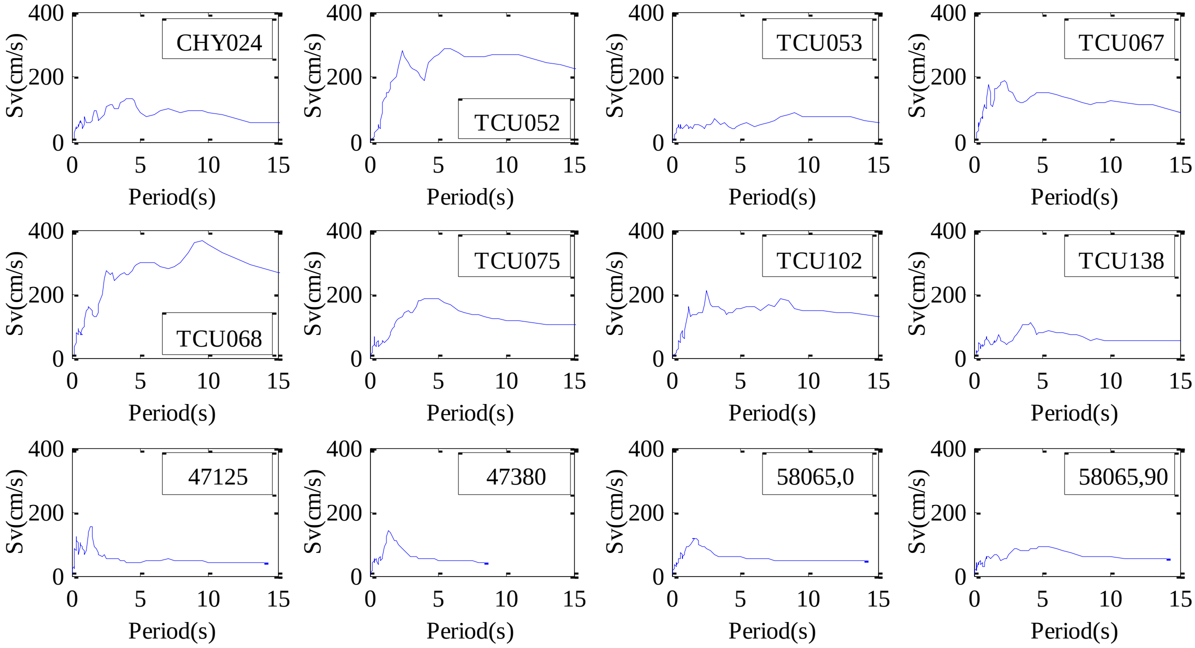


Figure 4. Spectral velocity of near-fault long-period ground motions. (Damping ratio = 5%)

## 4 ANALYSIS APPROACH AND RESULTS

A three-dimensional finite element model of the base-isolated building was developed in the commercial software ETABS, and nonlinear time history analysis was carried out. The RC framework was modelled by a total number of 3412 frame elements, and the basement exterior walls were modelled by 44 layered shell elements. Out-of-plane stiffness of the slabs was neglected, while the in-plane stiffness was accounted for by using rigid diaphragms. The rubber isolator element available in ETABS was used to model the LRBs and NRBs, in which a biaxial hysteretic model with coupled plasticity properties for two shear deformations was used to represent the horizontal force-deformation relationship. The selected twelve near-fault long-period ground motions and four ordinary motions were input into the model along X direction, and the peak ground acceleration of each record was scaled to 400 cm/s$^2$ according to current Chinese building code (GB 50011-2010). Rayleigh damping model was employed in the analysis, and the damping ratio was considered to be 0.05. Nonlinear time history analysis was carried out considering the Hilber-Hughes-Taylor method.

The seismic responses of the base-isolated model under near-fault long-period ground motions are compared to those obtained under ordinary motions. The peak story displacements and story shear forces under all the input ground motions are summarized in Table 3 and Table 4, respectively. The mean values of these two parameters are shown in Figure 5.

Table 3 summarizes the peak story displacements of the base-isolated structure under near-fault long-period and ordinary ground motions, and the mean values of peak story displacements under ordinary motions, Chi-Chi earthquake records, Loma Prieta earthquake records, and all selected near-fault long-period motions are presented in Figure 5. It can be seen that the maximum inter-story drift occurs at the base isolation layer, while the inter-story drifts in both superstructure and substructure are quite small. In addition, comparison of peak story displacements induced by ordinary and near-fault long-period ground motions demonstrates that near-fault long-period motions can induce particularly large story displacement on the base-isolated structure. The peak story displacement at the base isolation layer reaches a maximum value of 959 mm when the model is subjected to the ground motion at TCU052 station, while the peak story displacement only reaches 26 mm when the input ground motion is taken from Wenchuan earthquake record. Furthermore, the mean value of peak story displacements at the base isolation layer reaches 385 mm when the selected near-fault long-period motions are taken as input excitations, whereas the mean value is only 92 mm when the model is subjected to ordinary ground motions. The comparison of peak story displacements indicates that the base-isolated structure needs a higher seismic demand on the horizontal displacement of the base isolation layer when it is subjected to near-fault long-period ground motions.

**Table 3. Peak story displacements by ordinary and near-fault long-period motions (mm).**

| Story | EI Centro | Kobe | Taft | Wenchuan | CHY024 | TCU052 | TCU053 | TCU067 |
|---|---|---|---|---|---|---|---|---|
| 5 | 167 | 135 | 125 | 37 | 493 | 1115 | 188 | 395 |
| 4 | 164 | 132 | 123 | 37 | 487 | 1105 | 185 | 389 |
| 3 | 160 | 125 | 119 | 35 | 474 | 1078 | 177 | 377 |
| 2 | 153 | 116 | 112 | 32 | 454 | 1038 | 166 | 359 |
| 1 | 146 | 108 | 106 | 29 | 433 | 995 | 157 | 340 |
| BI | 140 | 102 | 101 | 26 | 417 | 959 | 150 | 326 |
| -1 | 0.19 | 0.21 | 0.20 | 0.16 | 0.54 | 1.16 | 0.29 | 0.38 |
| Base | 0 | 0 | 0 | 0 | 0 | 0 | 0 | 0 |

**Table 3. (Continued) Peak story displacements by ordinary and near-fault long-period motions (mm).**

| Story | 47125 | 47380 | 58065,0 | 58065,90 | TCU068 | TCU075 | TCU102 | TCU138 |
|---|---|---|---|---|---|---|---|---|
| 5 | 116 | 246 | 151 | 249 | 708 | 758 | 704 | 343 |
| 4 | 114 | 242 | 149 | 247 | 701 | 750 | 698 | 338 |
| 3 | 109 | 233 | 145 | 241 | 683 | 733 | 680 | 329 |
| 2 | 101 | 221 | 140 | 233 | 656 | 706 | 652 | 316 |
| 1 | 93 | 209 | 134 | 223 | 627 | 677 | 622 | 302 |
| BI | 87 | 199 | 129 | 214 | 604 | 652 | 598 | 291 |
| -1 | 0.23 | 0.29 | 0.24 | 0.36 | 0.75 | 0.81 | 0.72 | 0.41 |
| Base | 0 | 0 | 0 | 0 | 0 | 0 | 0 | 0 |

**Table 4. Peak story shear forces by ordinary and near-fault long-period motions ($10^3$ kN).**

| Story | EI Centro | Kobe | Taft | Wenchuan | CHY024 | TCU052 | TCU053 | TCU067 |
|---|---|---|---|---|---|---|---|---|
| 5 | 9.4 | 7.0 | 6.6 | 5.6 | 10.9 | 20.8 | 7.2 | 10.1 |
| 4 | 19.4 | 15.5 | 14.6 | 12.1 | 26.7 | 51.3 | 16.9 | 24.6 |
| 3 | 20.7 | 19.0 | 17.9 | 14.4 | 41.2 | 81.0 | 24.0 | 37.4 |
| 2 | 19.7 | 22.0 | 19.3 | 13.3 | 53.6 | 109.8 | 28.4 | 47.8 |
| 1 | 21.7 | 23.9 | 20.7 | 10.6 | 63.7 | 139.6 | 31.0 | 56.1 |
| BI | 27.5 | 24.5 | 24.8 | 12.2 | 73.0 | 172.6 | 32.9 | 63.3 |
| -1 | 52.6 | 36.3 | 38.5 | 38.3 | 91.8 | 178.7 | 54.6 | 65.8 |
| Base | 60.1 | 39.1 | 43.9 | 45.4 | 95.9 | 180.1 | 62.4 | 71.2 |

**Table 4. (Continued) Peak story shear forces by ordinary and near-fault long-period motions ($10^3$ kN).**

| Story | 47125 | 47380 | 58065,0 | 58065,90 | TCU068 | TCU075 | TCU102 | TCU138 |
|---|---|---|---|---|---|---|---|---|
| 5 | 7.0 | 8.3 | 5.4 | 5.8 | 13.5 | 14.8 | 14.4 | 9.6 |
| 4 | 15.5 | 19.6 | 12.6 | 14.3 | 33.4 | 36.1 | 35.6 | 22.8 |
| 3 | 19.9 | 28.1 | 17.9 | 22.5 | 53.1 | 56.0 | 55.9 | 33.2 |
| 2 | 20.1 | 33.0 | 21.4 | 30.0 | 72.2 | 75.0 | 74.8 | 39.9 |
| 1 | 17.5 | 36.5 | 24.6 | 36.7 | 91.1 | 95.7 | 92.6 | 46.1 |
| BI | 20.8 | 41.4 | 29.5 | 43.0 | 111.2 | 119.7 | 111.3 | 55.7 |
| -1 | 46.3 | 51.9 | 39.9 | 69.4 | 116.5 | 125.3 | 120.5 | 74.1 |
| Base | 54.4 | 55.7 | 44.2 | 76.7 | 117.5 | 126.6 | 122.4 | 79.3 |

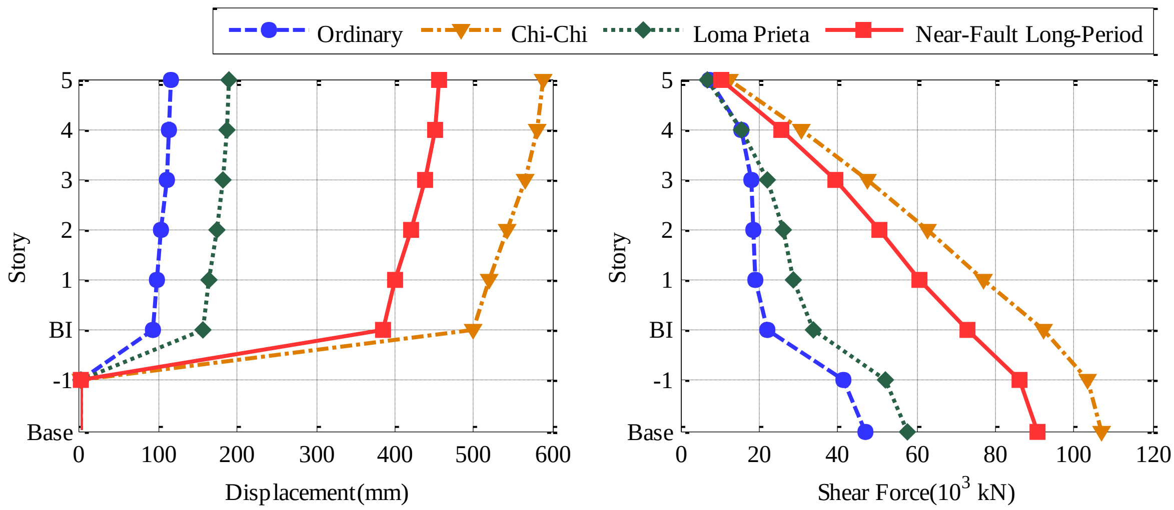


Figure 5. Comparison of mean values of peak story displacements and story shear forces induced by ordinary and near-fault long-period ground motions.

Table 4 summarizes the peak story shear forces of the base-isolated structure under near-fault long-period and ordinary ground motions, and the mean values of the peak story shear forces induced by ordinary motions, Chi-Chi earthquake records, Loma Prieta earthquake records, and all selected near-fault long-period motions are presented in Figure 5. The base shear forces are obtained by summing up all reaction forces at the column bases and shear wall bases. It is observed that story shear forces generally decrease with the height, and an obvious decrease in story shear forces can be noticed in the base isolation layer. Additionally, comparison of peak story shear forces generated by ordinary and near-fault long-period ground motions reveals that a larger force demand is expected when the base-isolated structure is subjected to near-fault long-period excitations. The peak base shear reaches a maximum value of 180,000 kN when subjected to the earthquake record at TCU052 station, while it is 39,000 kN when the model is excited by Kobe earthquake record. The mean value of peak base shears reaches 90,000 kN when the selected near-fault long-period motions are taken as input excitations, whereas the mean value is merely 47,000 kN when ordinary motions are considered. The comparison of peak story shear forces indicates that the ductility demand is highly expected when the base-isolated structure is subjected to near-fault long-period ground motions.

Figure 6 shows the restoring force characteristics in the base isolation layer under long-period and ordinary ground motions. Two types of coordinate ranges are used to show the force-displacement relationships. As shown in the figure, the force-displacement relationships of the base isolation layer can be characterized as bilinear hysteresis loops and are similar to the mechanical properties of Lead rubber bearings, indicating that the dynamic behavior of the base-isolated structure is considerably affected by rubber isolators. In addition, higher earthquake energy dissipation capacity of the base isolation layer is noticed when long-period ground motions are input into the structure. The energy dissipated by the base isolation layer is merely 568 kN·m when Wenchuan earthquake record is taken as the input excitation. However, the energy dissipation capacity of the base isolation layer reaches 29,188 kN·m when the earthquake record at TCU052 station is input into the model. The increase of dissipated energy in the base isolation layer indicates that resonant behavior occurs when near-fault long-period motions are input into the model, and high energy dissipation capacity of the isolation layer is expected when the base-isolated structure is subjected to near-fault long-period ground motions.

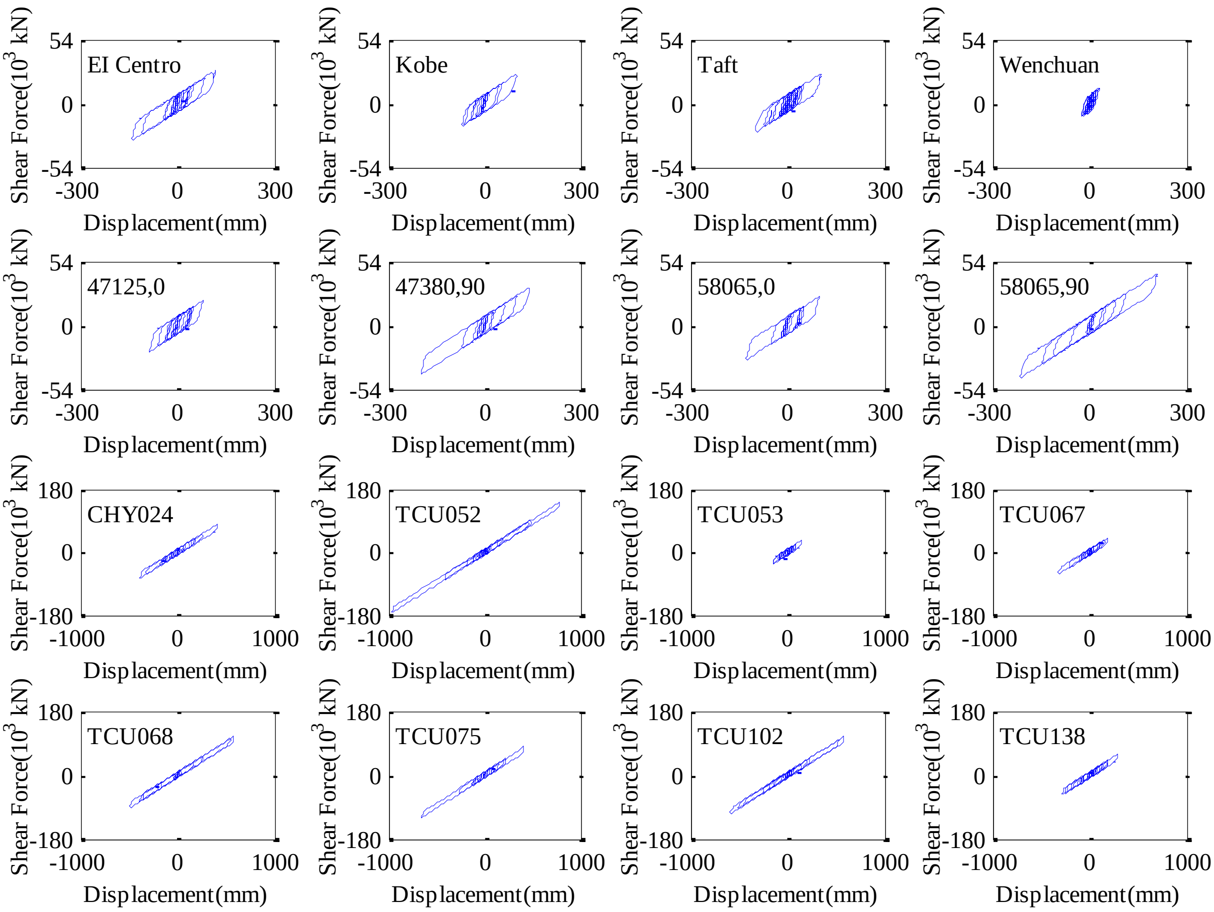


Figure 6. Restoring force characteristics in the base isolation layer.

## 5 CONCLUSIONS

Evaluation of seismic performance of seismically isolated structures subjected to long-period ground motions is one important aspect in structural design. In this study, the nonlinear seismic responses of a base-isolated hospital building subjected to near-fault long-period ground motions are compared with those of ordinary ground motions. Twelve near-fault long-period ground motions are selected from Chi-Chi earthquake and Loma Prieta earthquake records, and the effects of long-period ground motions on peak story displacements, peak story shear forces, and energy dissipation capacity of the base isolation layer are evaluated afterwards. The analysis results demonstrate that near-fault long-period ground motions can induce particularly large story displacements and story shear forces on the base-isolated structure, and more input energy is consumed by the base isolation layer under long-period ground motions. The results indicate that the base-isolated structure needs higher seismic demands when subjected to near-fault long-period ground motions, and the design provisions in current seismic codes have underestimated the seismic responses because only ordinary far-fault ground motions are considered in the seismic codes. Finally, it is important for structural engineers to realize that seismically isolated structures are vulnerable to near-fault long-period ground motions and it is necessary to provide them with adequate countermeasures.

## REFERENCES


Dicleli, M. & Buddaram, S. (2007). Equivalent Linear Analysis of Seismic-Isolated Bridges Subjected to Near-Fault Ground Motions with Forward Rupture Directivity Effect. *Engineering Structures*, Vol 29(1) 21-32.

GB 50011-2010. (2010). Code for Seismic Design of Buildings. Beijing: China Architecture & Building Press.

Hall, J.F., Heaton, T.H., Halling, M.W. & Wald, D.J. 1995. Near-Source Ground Motion and Its Effects on Flexible Buildings. *Earthquake Spectra*, Vol 11(4) 569-605.

Heaton, T.H., Hall, J.F., Wald, D.J. & Halling, M.W. (1995). Response of High-Rise and Base-Isolated Buildings to A Hypothetical MW 7.0 Blind Thrust Earthquake. *Science*, Vol 267(5195) 206-11.

Jangid, R.S. & Kelly, J.M. (2001). Base Isolation for Near-Fault Ground Motion. *Earthquake Engineering and Structural Dynamics*, Vol 30(5) 691-707.

Liao, W.I., Loh, C.H. & Lee, B.H. (2004). Comparison of Dynamic Response of Isolated and Non-Isolated Continuous Girder Bridges Subjected to Near-Fault Ground Motions. *Engineering Structures*, Vol 26(1) 2173-83.

Malhotra, P.K. (1999). Response of Buildings to Near-Field Pulse-Like Ground Motions. *Earthquake Engineering and Structural Dynamics*, Vol 28(11) 1309-26.

Mazza, F. & Vulcano, A. (2012). Effects of Near-Fault Ground Motions on the Nonlinear Dynamic Response of Base-Isolated R.C. Framed Buildings. *Earthquake Engineering and Structural Dynamics*, Vol 41(2) 211-32.

Shekari, M.R., Khaji, N. & Ahmadi, M.T. (2010). On the Seismic Behavior of Cylindrical Base-Isolated Liquid Storage Tanks Excited by Long-Period Ground Motions. Soil Dynamics and Earthquake Engineering, Vol 30(10) 968-80.